Acoustic and Seismic Array Processing in Sensor Network

Kung Yao
UCLA

CTW, May 23, 2006

Outline

0. Introduction
1. Source localization using randomly distrib. arrays based on TDOA-LS methods
2. Source localization of near/far field sources based on AML method
3. Near field seismic source localization using accelerometric data
4. Distributed sensor node localization
5. Conclusions
6. Challenging Problems

0. Introduction

- The purpose of a sensor network is to sense one or more specific physical phenomena
- Often it is necessary to detect, track, localize, classify these physical sources
- We consider three different approaches for acoustic and seismic source localization
- Often it is also necessary to localize the sensing nodes/arrays relative to the sources
- We also consider a distributed Gauss-Newton iterative node localization method

1. Randomly distributed array processing based on TDOA-LS methods

Coherent Processing for Narrowband Beamforming

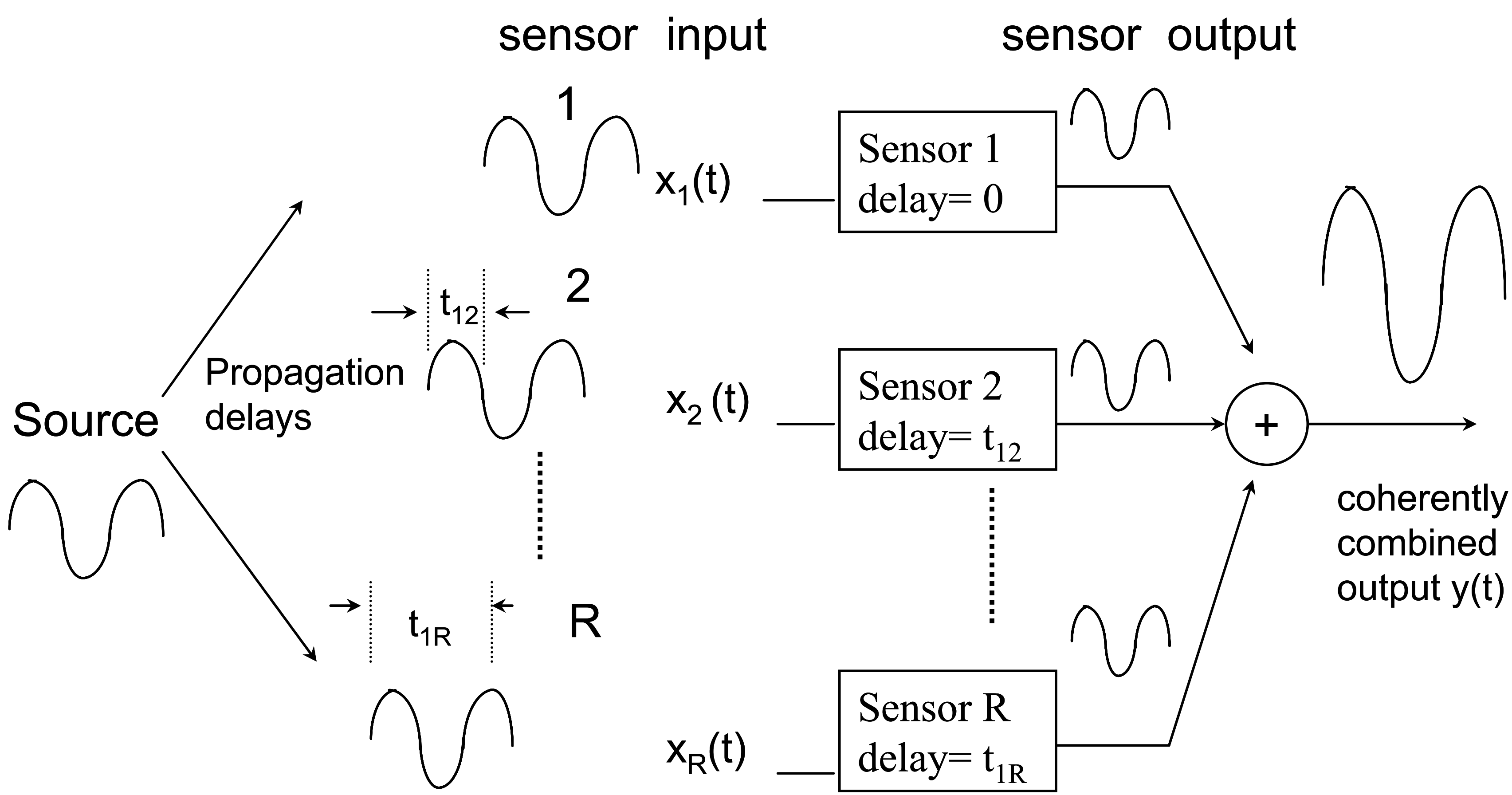

Space-Time-Frequency Wideband Beamforming

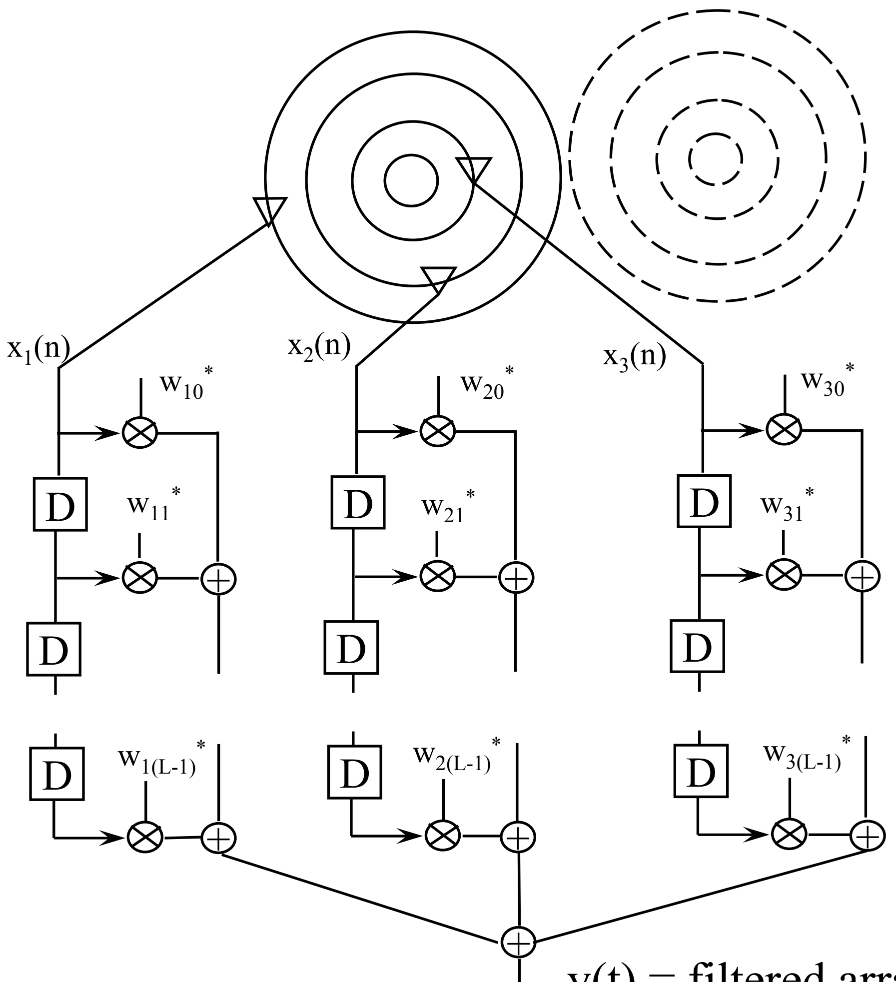

y(t) = filtered array output

Data from D number of sources collected by N randomly distributed sensors

$$x_n(t) = \sum_{d=1}^{D} s_d(t - t_{d,n}) + m_n(t)$$

Output of the beamformer

$$y(t) = \sum_{n=1}^{N} \sum_{l=0}^{L-1} w_{nl}^* x_n(t-l)$$

$t_{d,n}$ - time-delay

L - number of FIR taps

w - array weight

Array Weight Obtained by Dominant Eigenvector of Cross-Correlation Matrix

(For simplicity, consider N = 3)

Sample Auto- and Cross-Correlation Matrices

$$
\begin{aligned}
\mathbf{R}_L^{11} &= E\mathbf{x}_1\mathbf{x}_1^H = E\mathbf{x}_2\mathbf{x}_2^H = E\mathbf{x}_3\mathbf{x}_3^H \\
\mathbf{R}_L^{12} &= E\mathbf{x}_1\mathbf{x}_2^H, \qquad \mathbf{R}_L^{21} = \mathbf{R}_L^{12H} \\
\mathbf{R}_L^{13} &= E\mathbf{x}_1\mathbf{x}_3^H, \qquad \mathbf{R}_L^{31} = \mathbf{R}_L^{13H} \\
\mathbf{R}_L^{23} &= E\mathbf{x}_2\mathbf{x}_3^H, \qquad \mathbf{R}_L^{32} = \mathbf{R}_L^{23H} \\
\mathbf{R}_{3L} &= E\mathbf{x}\mathbf{x}^H = \begin{bmatrix} \mathbf{R}_L^{11} & \mathbf{R}_L^{12} & \mathbf{R}_L^{13} \\ \mathbf{R}_L^{12H} & \mathbf{R}_L^{11} & \mathbf{R}_L^{23} \\ \mathbf{R}_L^{13H} & \mathbf{R}_L^{23H} & \mathbf{R}_L^{11} \end{bmatrix}
\end{aligned}
$$

Maximizing Beamformer Output $\max\limits_{\|\mathbf{w}_{3L}\|=1} \{\mathbf{w}_{3L}^H \mathbf{R}_{3L} \mathbf{w}_{3L}\}$

where $\mathbf{w}_{3L} = [w_{10}, w_{11}, \ldots, w_{1(L-1)}, \ldots, w_{20}, \ldots, w_{2(L-1)}, \ldots, w_{30}, \ldots, w_{3(L-1)}]^T$ is the eigenvector of largest eigenvalue of $\mathbf{R}_{3L}\mathbf{w}_{3L} = \lambda_{3L}\mathbf{w}_{3L}$

Time delays $t_{d,\,n}$ est. from the $\mathbf{w}_{3L}$ (Yao et al, IEEE JSAC, Oct. 1998)

Intuitive & Formal Interpretation of the Beamformer

Intuitive interpretation

Max array output ~ coherently sum the "strongest part" of the source

Szego asymptotic distribution of eigenvalues (1915)

$$\int_{-0.5}^{0.5} \boldsymbol{S}(\omega)\,\boldsymbol{d}\omega = \lim_{L\to\infty} \frac{\lambda_1^{(L)} + \ldots + \lambda_L^{(L)}}{L}$$

$$\boldsymbol{S}_{\max} = \int_{-0.5}^{0.5} \max\{\boldsymbol{S}(\omega)\}\,\boldsymbol{d}\omega = \lim_{L\to\infty} \lambda_L^{(L)}$$

$$\approx \lambda_L^{(L)} = \max_{\|\boldsymbol{w}_L\|=1} \{\boldsymbol{w}_L^H \boldsymbol{R}_L \boldsymbol{w}_L\}$$ for sufficiently large L

Simple Example

- Second order AR source with spectral peak at f = 0.2
- $t_{12} = 3$; $t_{23} = 2$; $t_{13} = 5$
- Array $w_L^{(r)} = \phi_{3L}^{(3L)}(rL : -1 : (r-1)L+1)$, $r = 1, 2, 3.$
- Propagation delay information contained in the array weights $w_L^{(r)}$
- Each array FIR acts as a narrowband filter centered at frequency of S_{max}

Continuing

Values of $|w_L^{(1)}|$, $|w_L^{(2)}|$ and $|w_L^{(3)}|$

n	$\lvert w_L^{(1)}\rvert$	$\lvert w_L^{(2)}\rvert$	$\lvert w_L^{(3)}\rvert$
1	0.0062	0.0011	0.0002
2	0.0088	0.0020	0.0005
3	0.0114	0.0036	0.0011
4	0.0140	0.0062	0.0020
5	0.0165	0.0088	0.0036
6	0.0191	0.0114	0.0062
7	0.0216	0.0140	0.0088
8	0.0241	0.0165	0.0114
9	0.0266	0.0191	0.0140
10	0.0291	0.0216	0.0165
11	0.0315	0.0241	0.0191
12	0.0339	0.0266	0.0216
13	0.0363	0.0291	0.0241
14	0.0386	0.0315	0.0266
15	0.0409	0.0339	0.0291

Mag. of three array weights

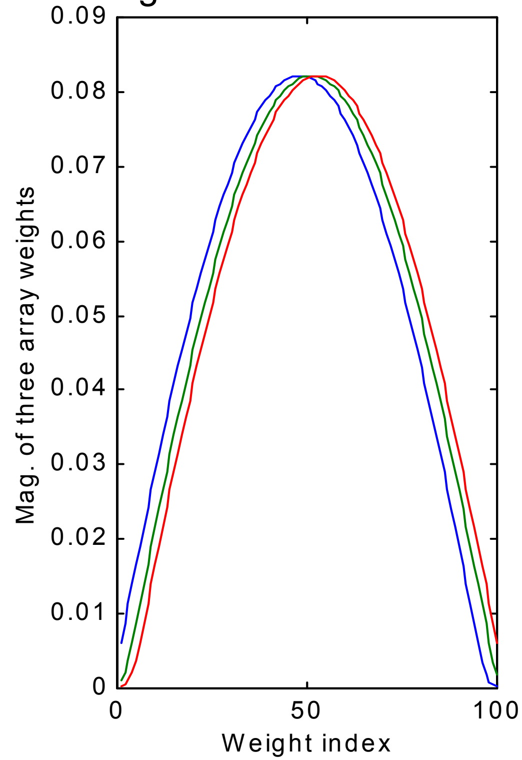

Mag. of transfer function of any array channel vs. freq

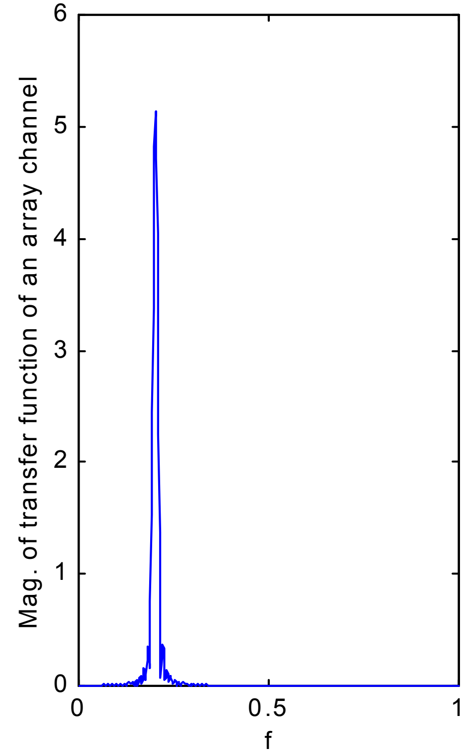

Source Localization from Estimated Time Difference of Arrival (TDOA)

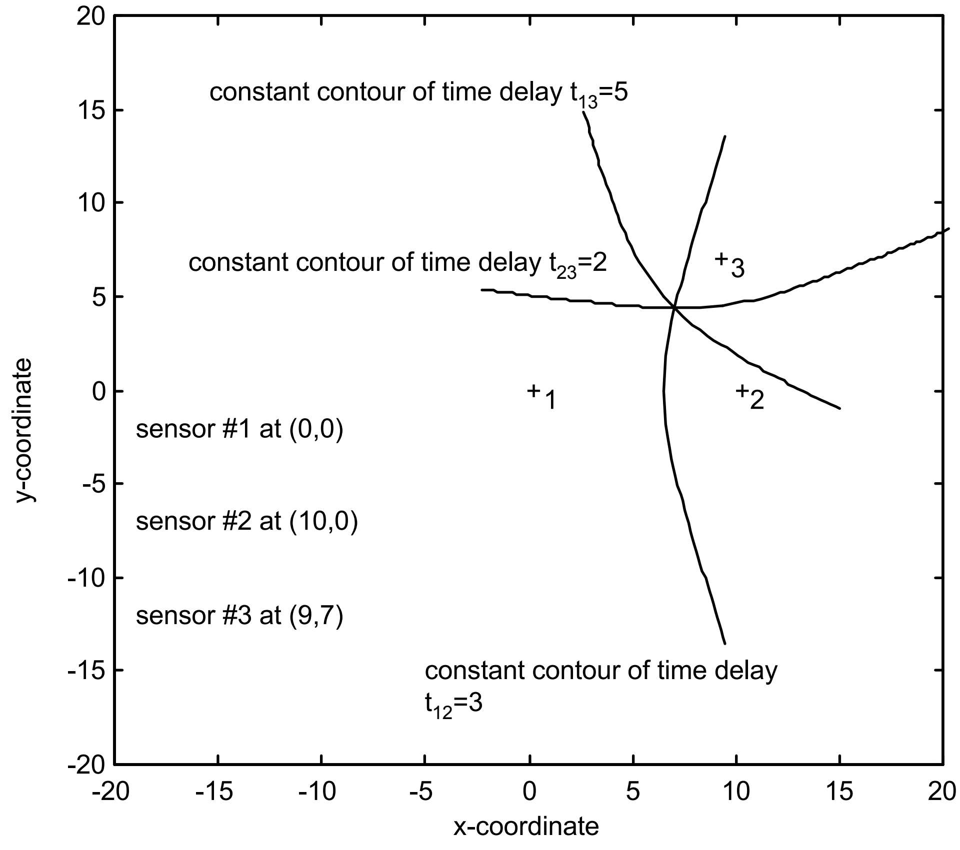

TDOA - Least-Squares

- Least-squares solution is then given as follows after algebraic manipulation

We write $Aw = b$, where

$$A = \begin{bmatrix} x_2 & y_2 & z_2 & -t_{12} & t_{12}^2/2 \\ x_3 & y_3 & z_3 & -t_{13} & t_{13}^2/2 \\ \vdots & \vdots & \vdots & \vdots & \vdots \\ x_n & y_n & z_n & -t_{1n} & t_{1n}^2/2 \end{bmatrix}, w = \begin{bmatrix} x_t \\ y_t \\ z_t \\ vs_1 \\ v^2 \end{bmatrix}, b = \frac{1}{2}\begin{bmatrix} r_2^2 \\ r_3^2 \\ \vdots \\ r_n^2 \end{bmatrix}$$

An overdetermined solution of the source location and speed of propagation can be given from the sensor data as follows

$\hat{w} = A^+ b$, where the pseudoinverse $A^+ = (A^T A)^{-1} A^T$

Source Localization and Speed of Propagation Results Using Seismic Array Sensors

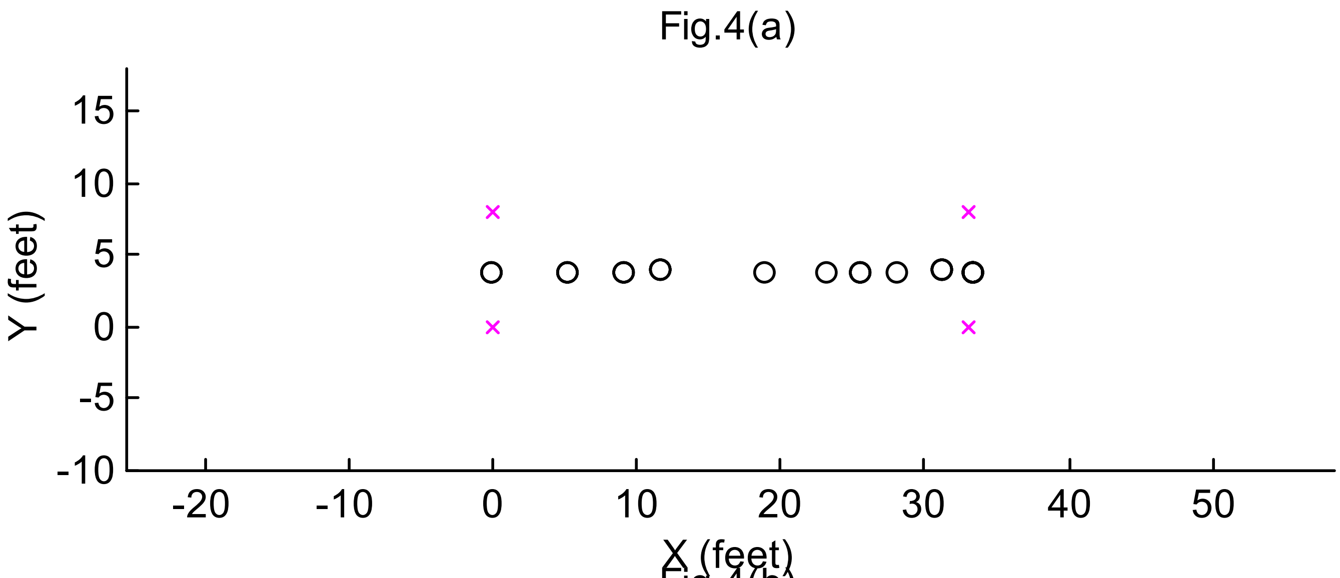

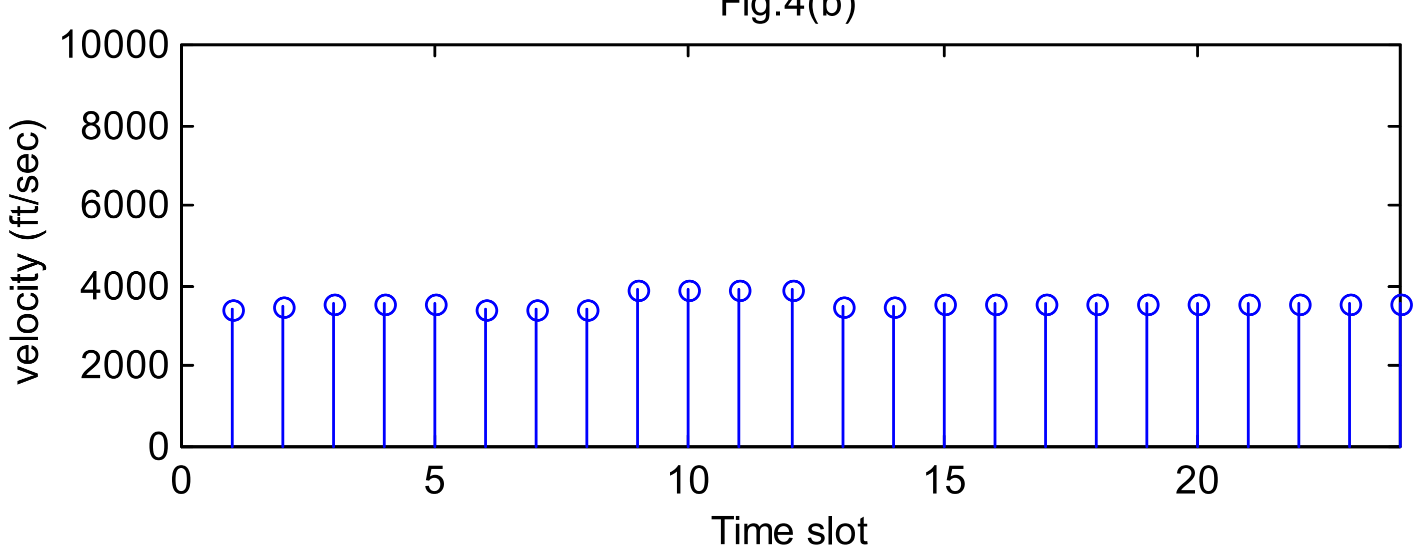

2. Approx. ML Estimation Method

- ML method is a well-known statistical est. tool
- We formulated an approx. ML (**AML**) method for wideband signal for DOA, source localization, and optimal sensor placement in the freq. domain (Chen-Hudson-Yao, IEEE Trans. SP, Aug. 2002)
- AML method generally outperforms many suboptimal techniques such as closed-form least squares and wideband MUSIC solutions
- Has relative high complexity

AML Metric Plot

- Peak at source location in near-field case
- Broad "lobe" along source direction in far-field case
- Sampling frequency f_s = 1KHz, SNR = 20dB

Near-field case

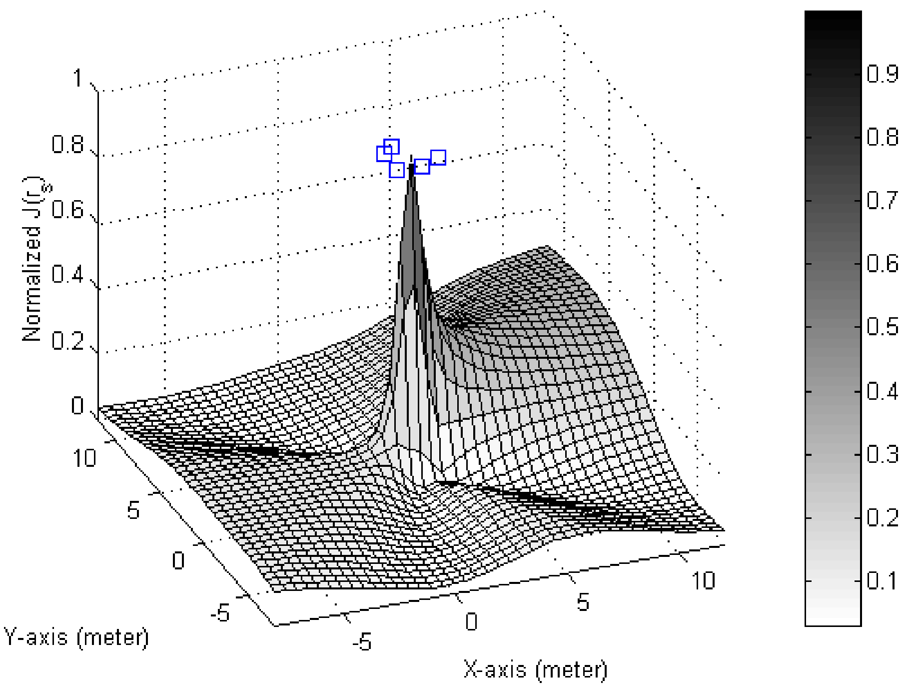

Far-field case

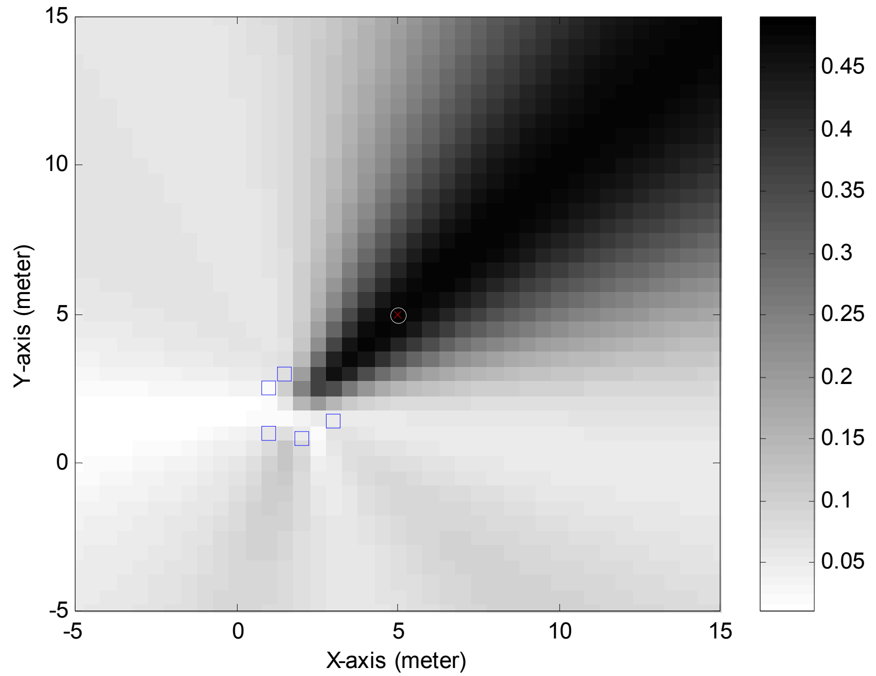

□ – sensor locations

Semi-Anechoic Room at Xerox Parc

Indoor Convex Hull Exp. Results

- Semi-anechoic room, SNR = 12dB
- Direct localization of an omni-directional loud speaker playing the LAV (light wheeled vehicle) sound
- AML RMS error of 73 cm, TOA-LS RMS error of 127cm

AML

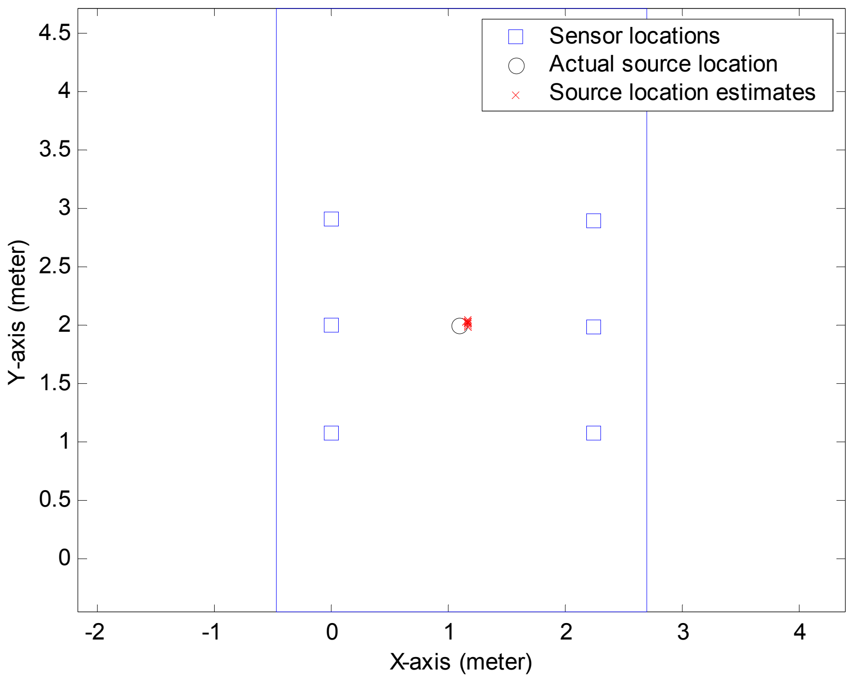

LS

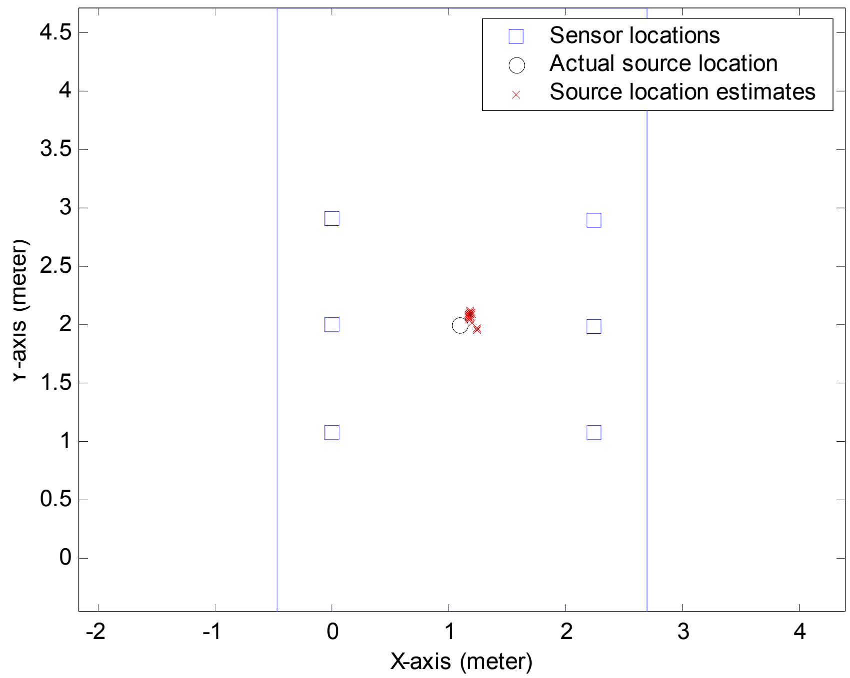

Outdoor Testing at Xerox -Parc

Outdoor Moving Source Exp. Results

- Omni-directional loud speaker playing the LAV sound while moving from north to south
- Far-field situation: cross-bearing of DOAs from three subarrays

AML

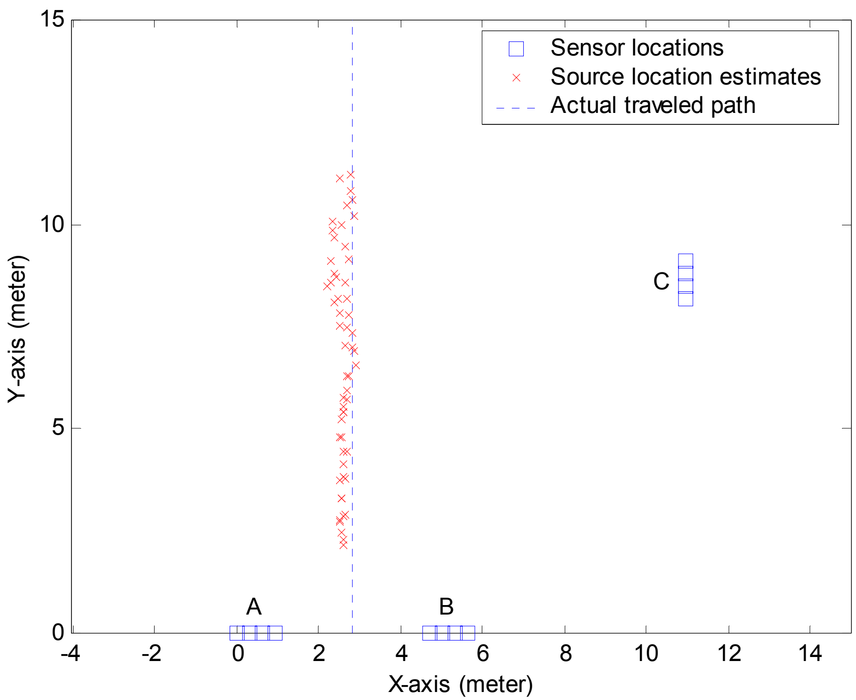

LS

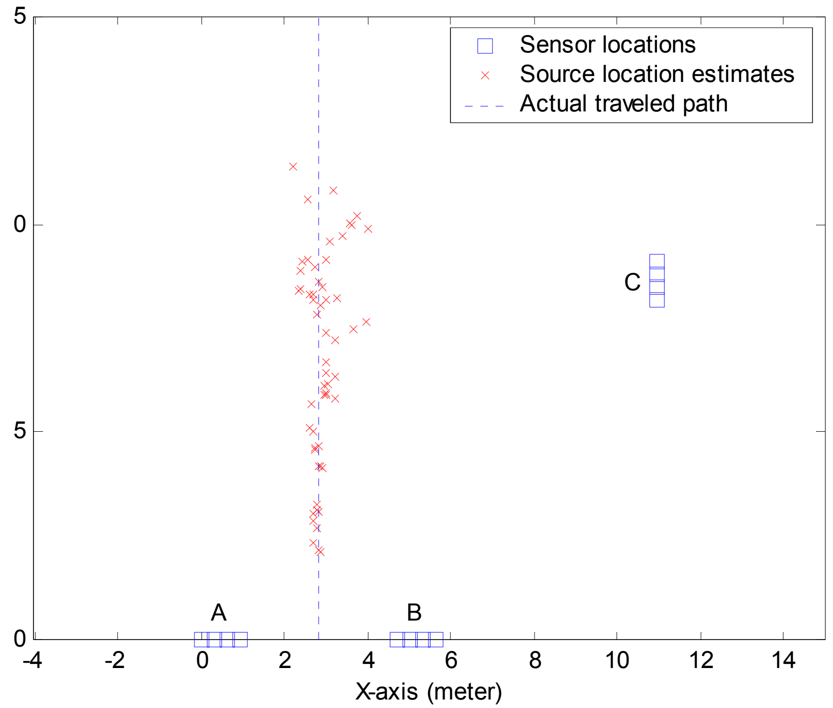

Optimum Sensor Placement via CRB Approach

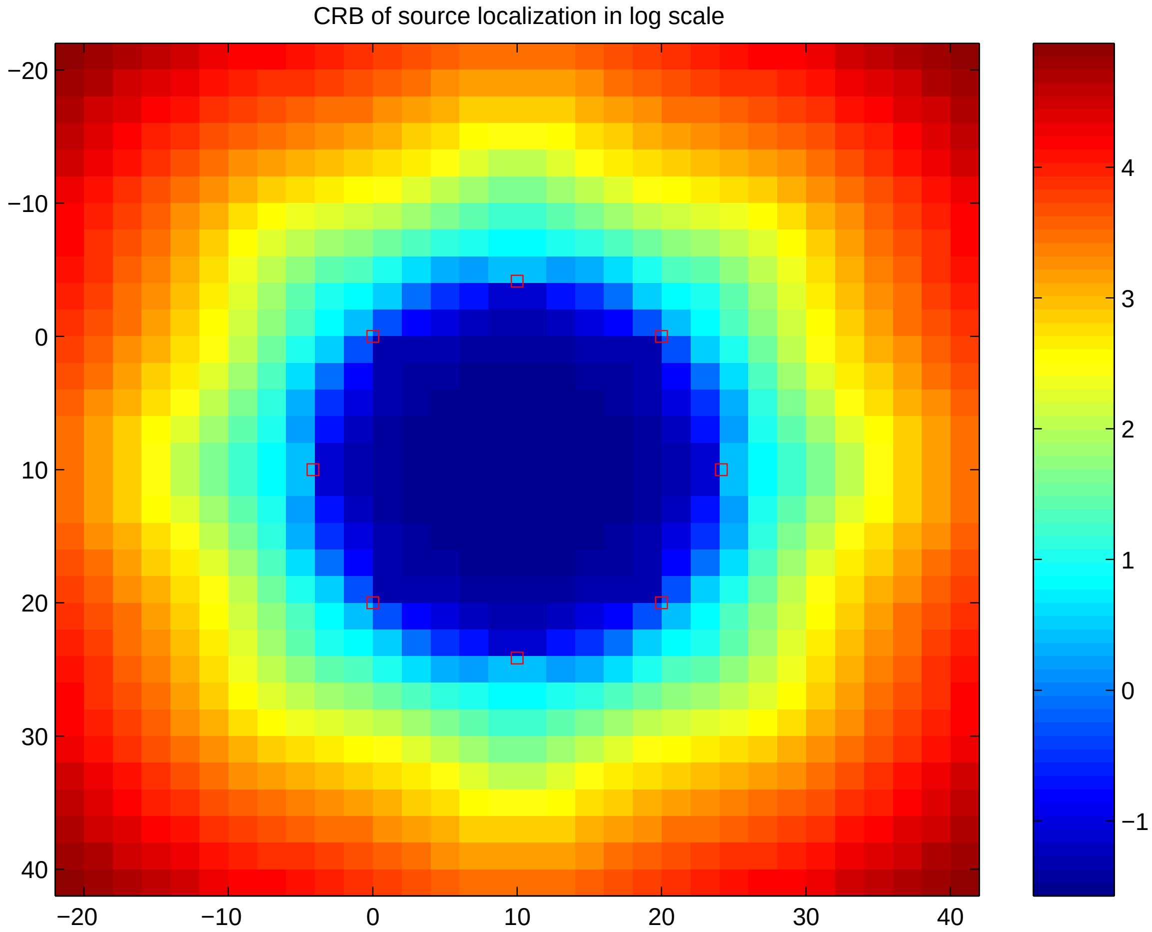

High CRB value

Low CRB value

Source should be inside the convex hull of the sensors

Sensor Network at 29 Palms

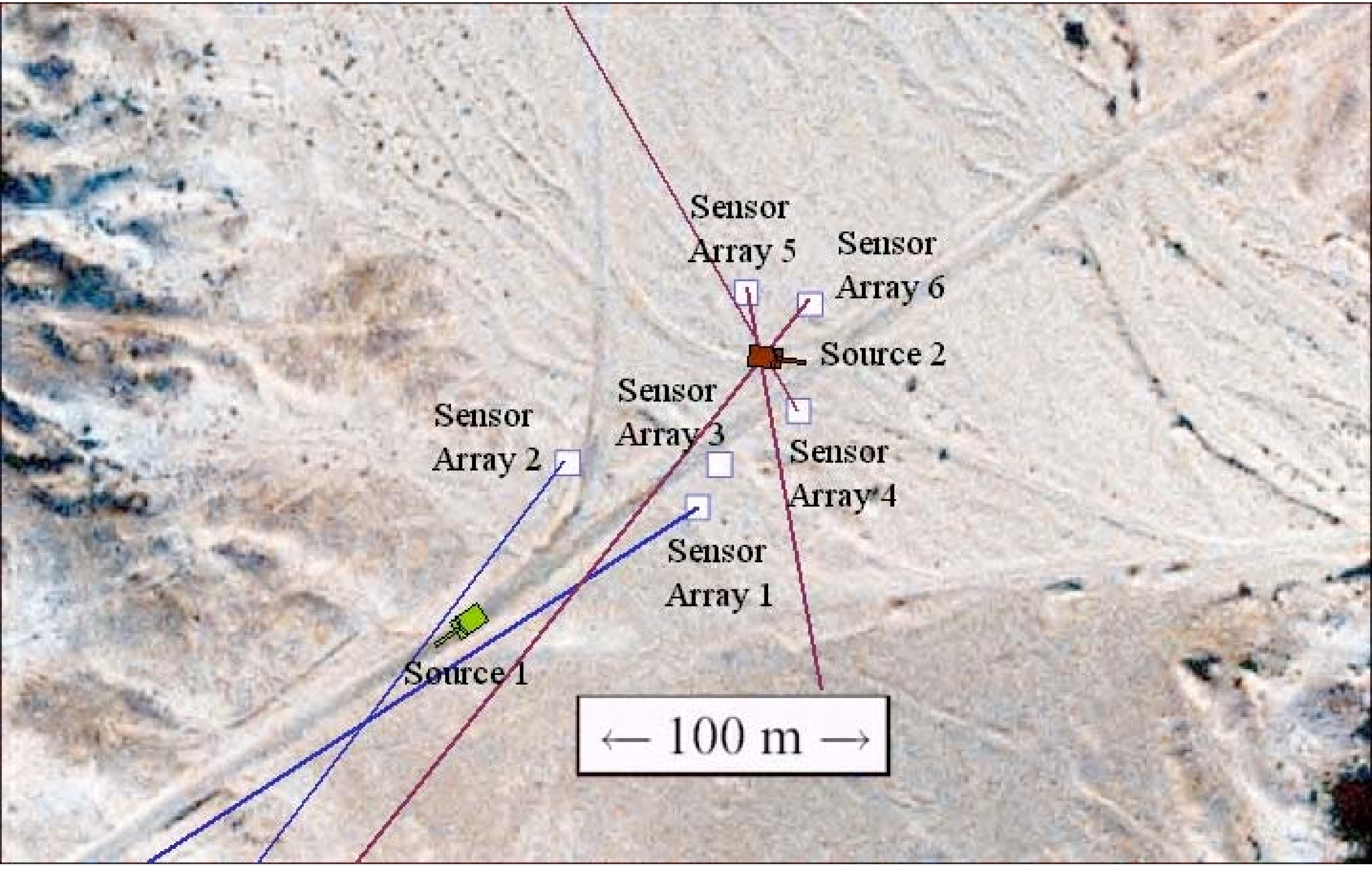

29 Palms Field Measurement

- Single Armored Amphibious Vehicle (AAV) traveling at 15mph
- Far-field situation: cross-bearing of DOAs from two subarrays (square array of four microphones, 1ft spacing)

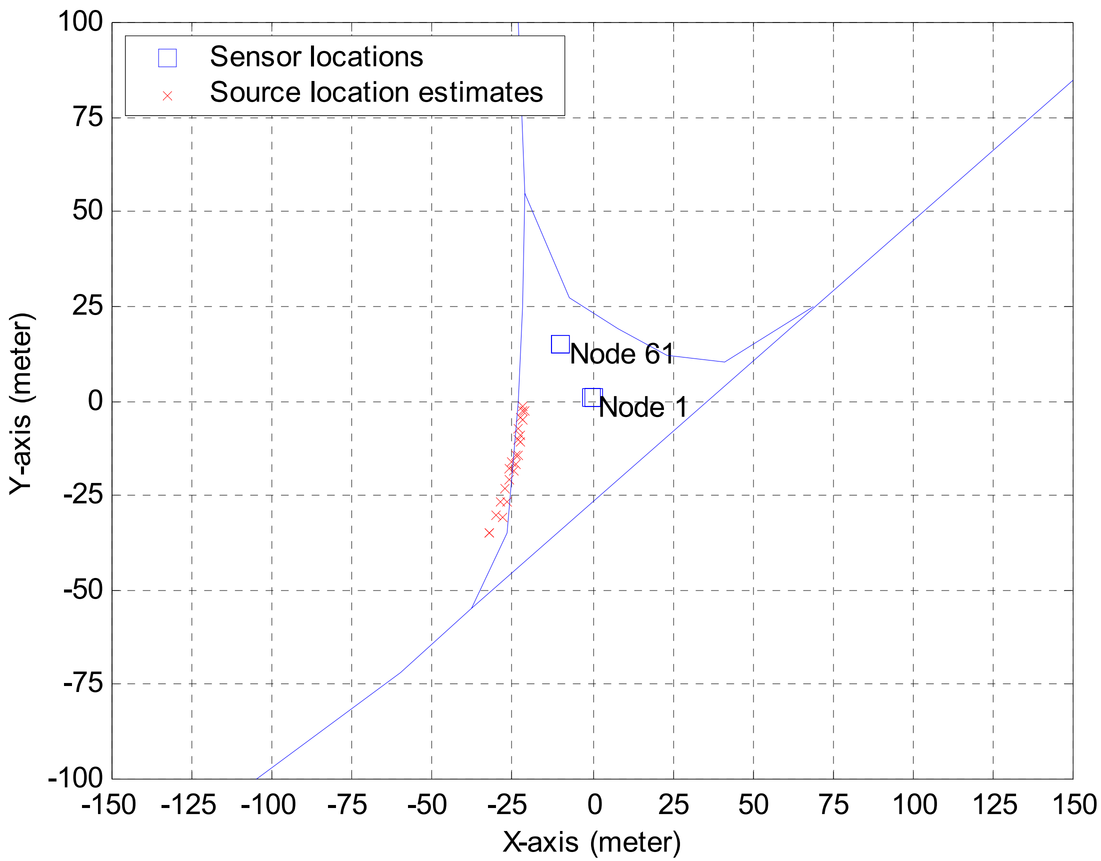

Outdoor Experiment using iPAQ testbed

One and Two Source AML Localization

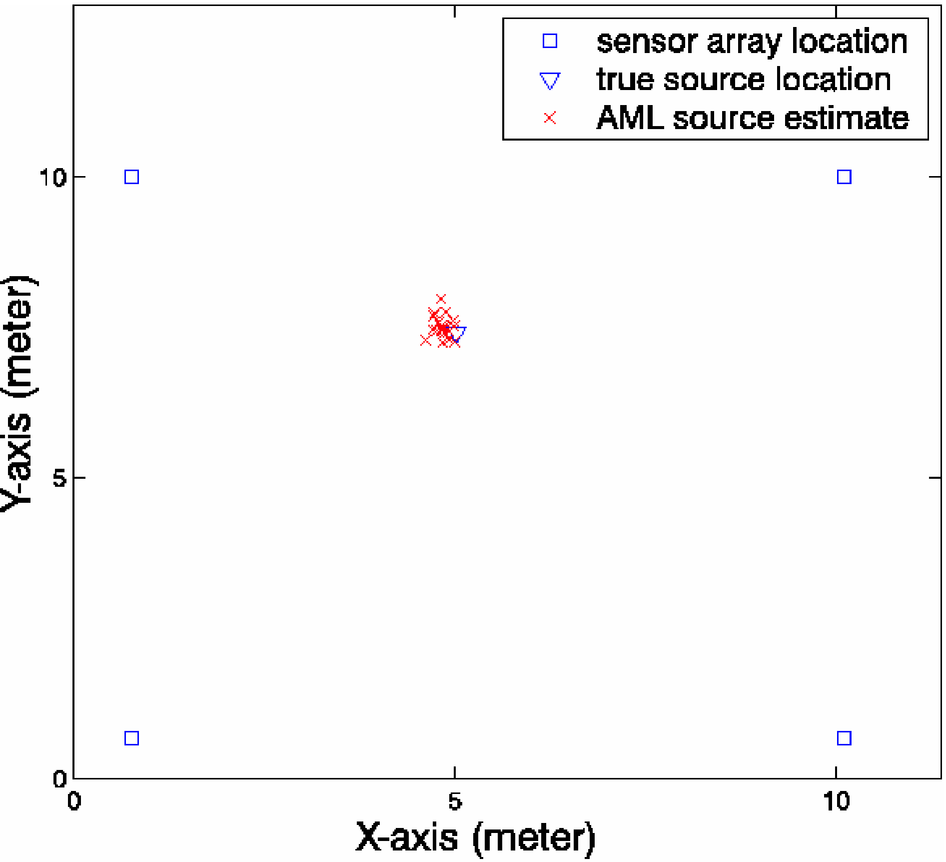

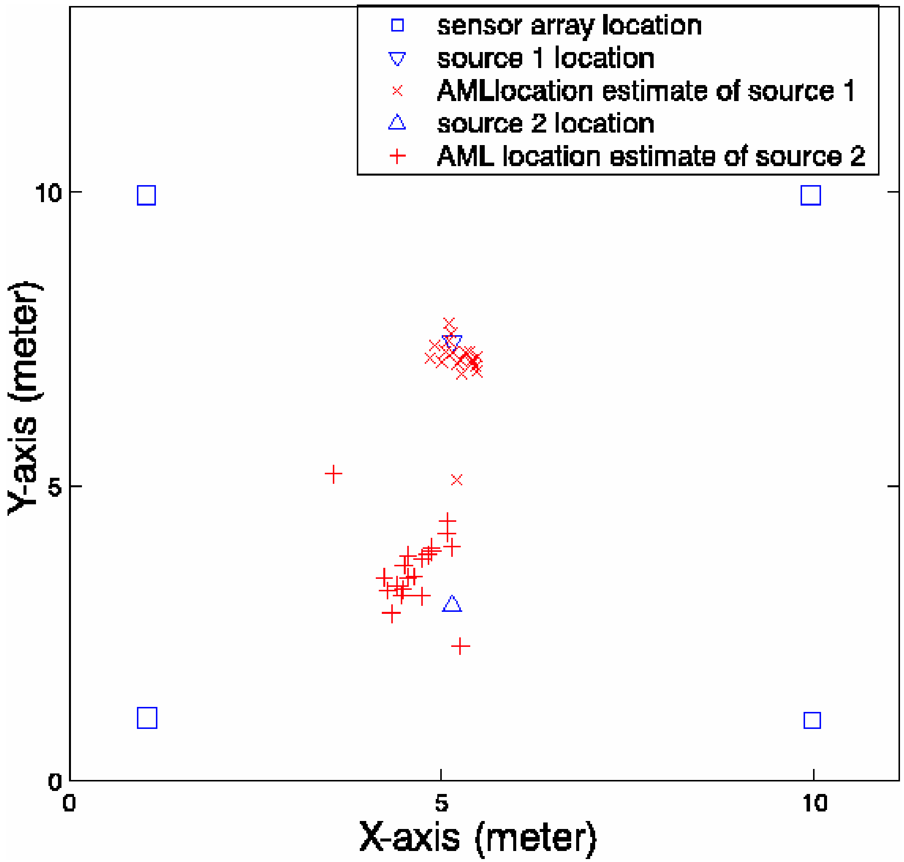

Space-Frequency Classification of Targets

- Previous discussions show that AML is able to estimate the DOAs of multiple targets
- Then the targets are spatially separated, detected, and located
- Since the AML algorithm not only estimates the DOA spatially, but also can yield the dominant spectral contents of each target
- The spectral signature of the target at a given DOA can provide information for classification

Spectra of Two Targets Used in Simulation for AML DOA Estimation

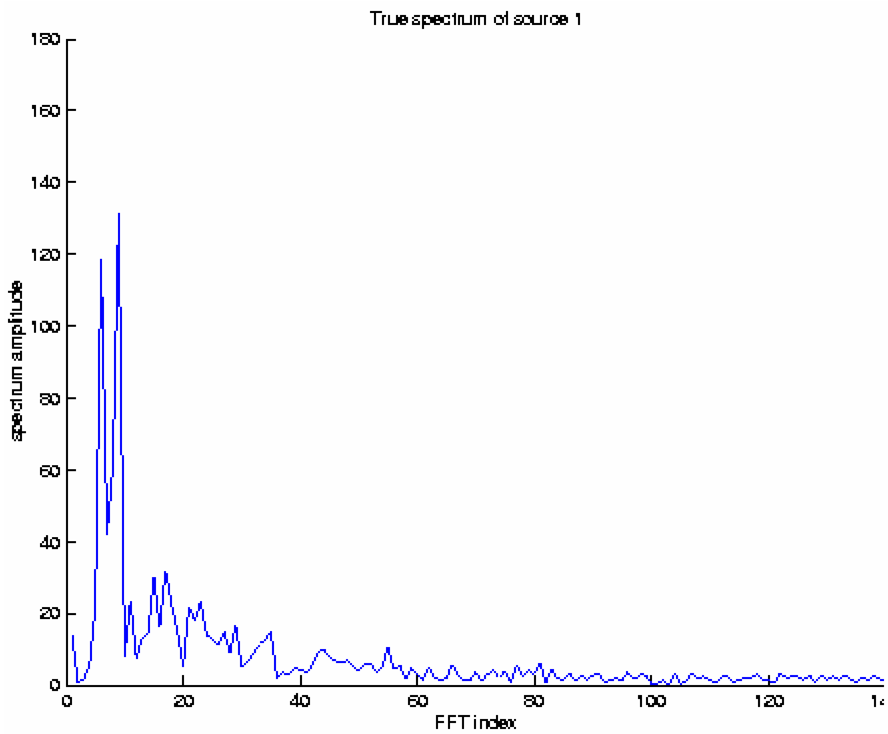

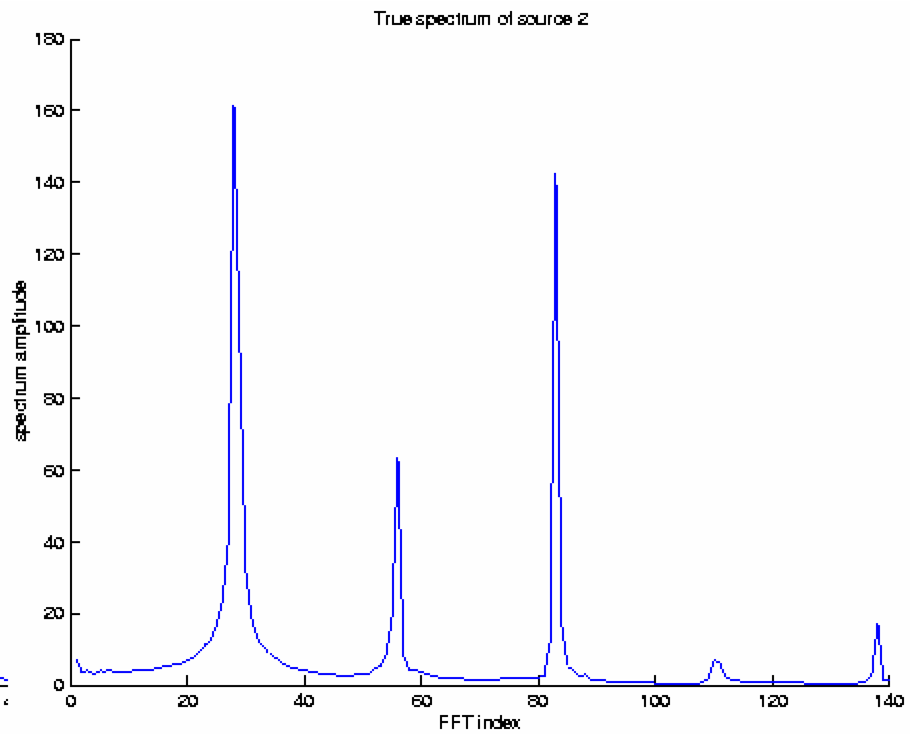

One FFT index no. = 14 Hz

Tracked vehicle data **Simple sound data**

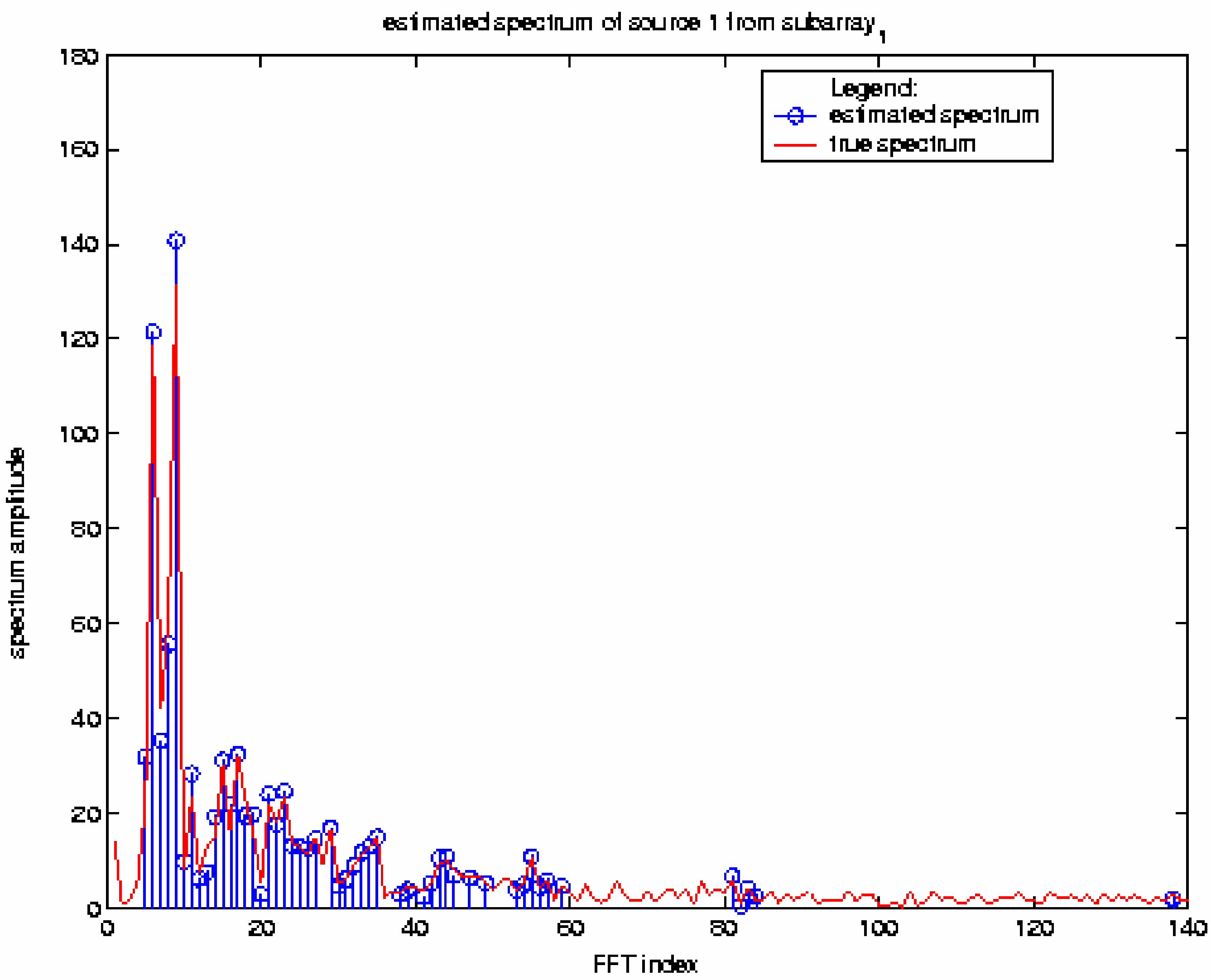

Excellent estimation of spectrum of source 1 at subarray 1

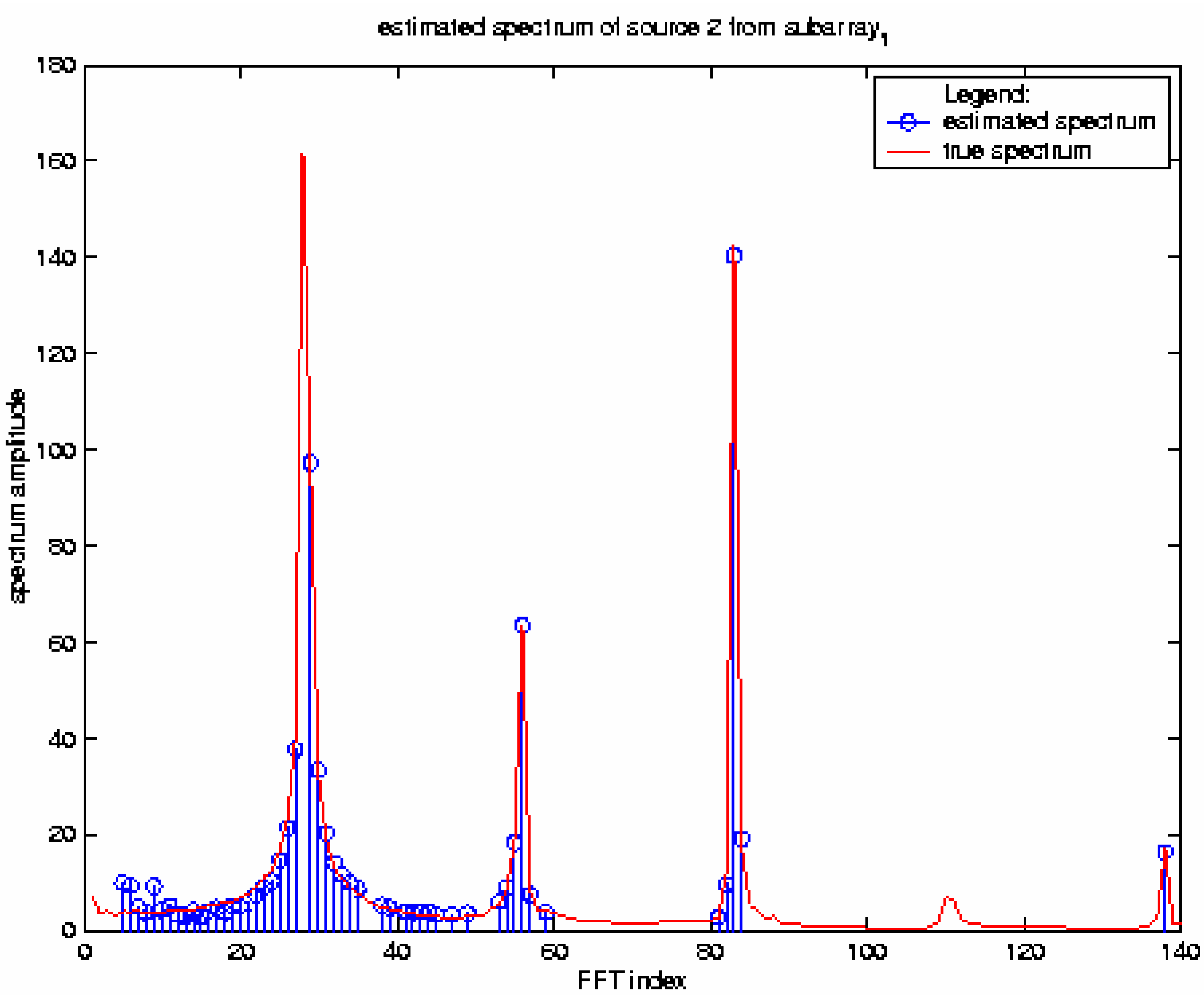

Excellent estimation of spectrum of source 2 at subarray 1

Other Use of AML Algorithm

- We are using the AML algorithm to detect, localize, and classify woodpeckers in collaboration with bio-complexity researchers
- We are using the AML metric as the LR function in the recursive formulation of particle filtering approach for real-time tracking of a human speaker in a reverberant room

Tracking Experiment

Tracking experiments in a reverberant room

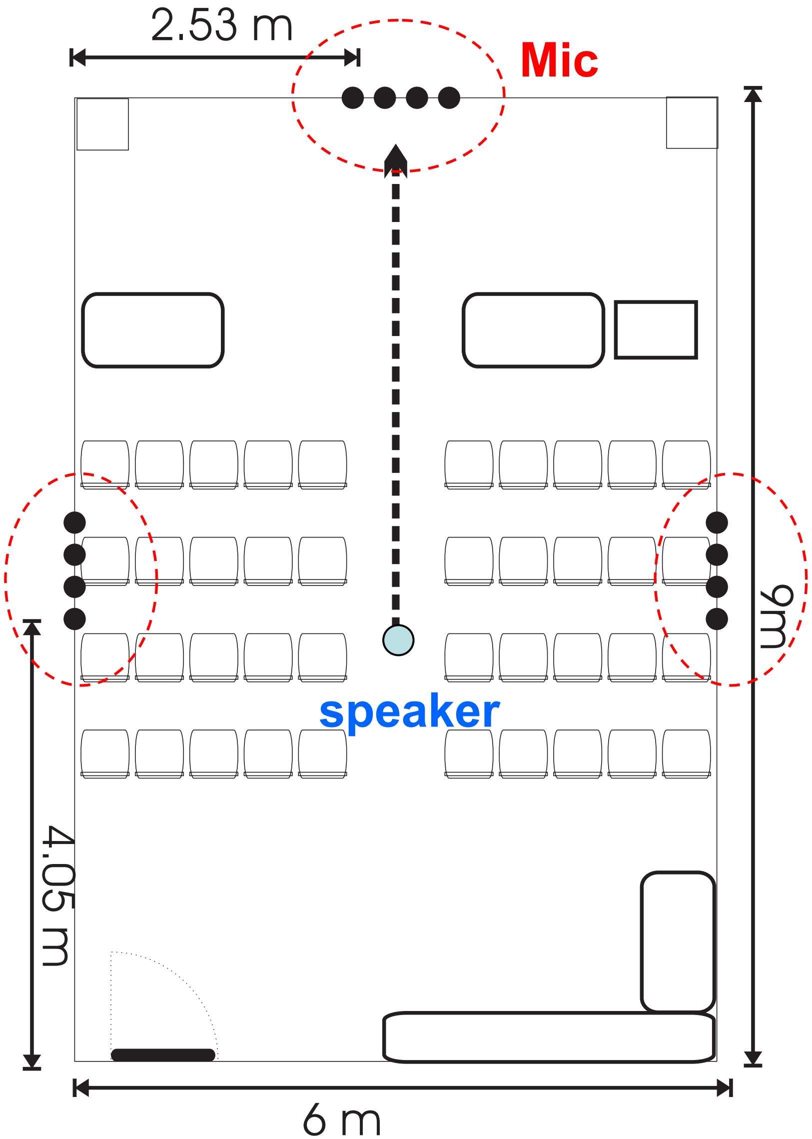

Experimental Results

Tracking Results in x-axis

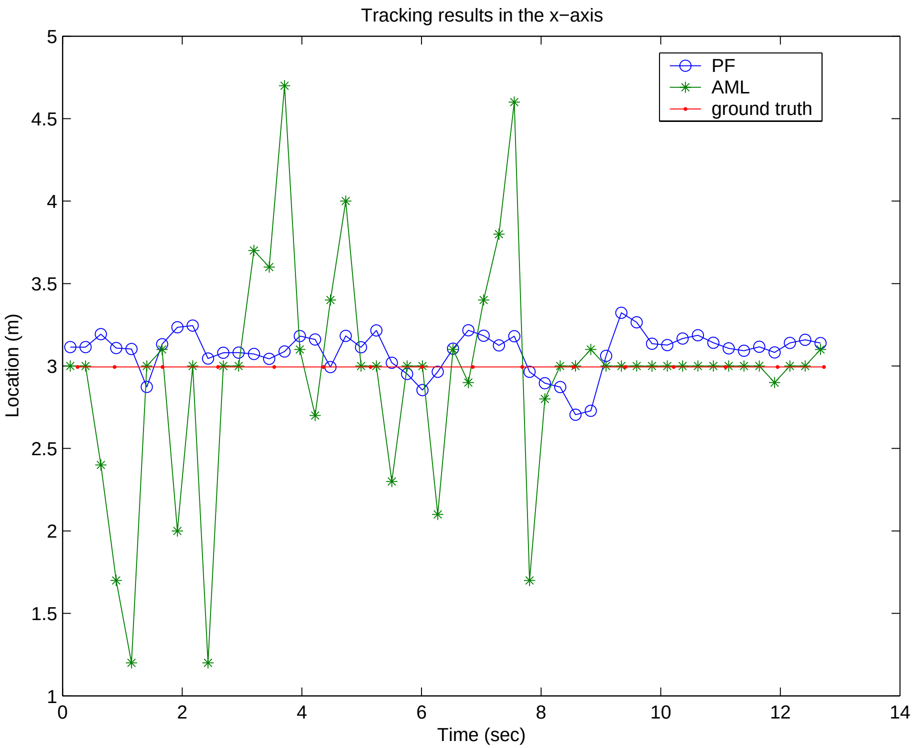

Tracking Results in y-axis

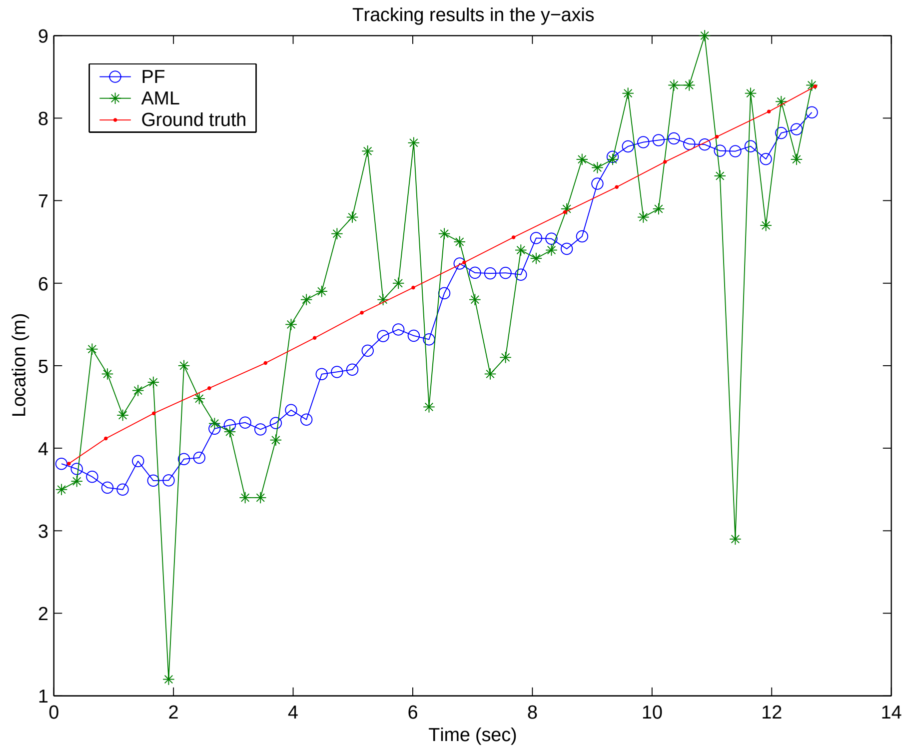

Update rate: 128 ms, # of particles=200

3. Garner Valley, CA
Acoustic Array Experiment

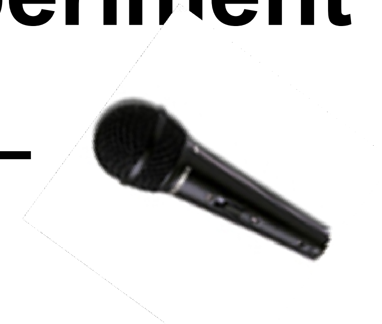

- **8 low cost Behringer XM200S microphones**
- **Each array consists of 4 microphones 1 meter apart in a square**

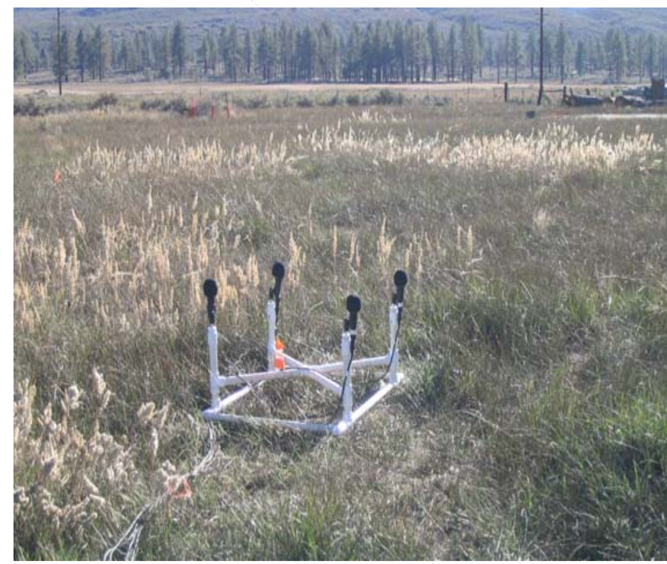

- **2 acoustic arrays**
- **The output of 8 microphones are sent to the Presonus Firepod 8 channel 94bit/96kb firewire-based recording sys.**
- **The recording system synchronizes the acoustic signals and sends to a PC for AML-based DOA/loc. algorithm**

Garner Valley, CA
Seismic Array Experiment

- **Episensor tri-axial/bi-axial accelerometer sensors**
- **Accelerometers have wide frequency/amplitude ranges, and wide dynamic range**
- **Outputs of accelerometers are fed to the low power, high resolution Quanterra Q330s recording systems**
- **9 sensor (6 tri-axial and 3 bi-axial), 8 of them on the perimeter of a 100 feet square, and the last one in the center**

Garner Valley Acoustic and Seismic Field Measurements/Results

- Metal hammer struck a heavy metal plate at the two separate locations

Acoustic and Seismic Sensor Map **Acoustic Array Map**

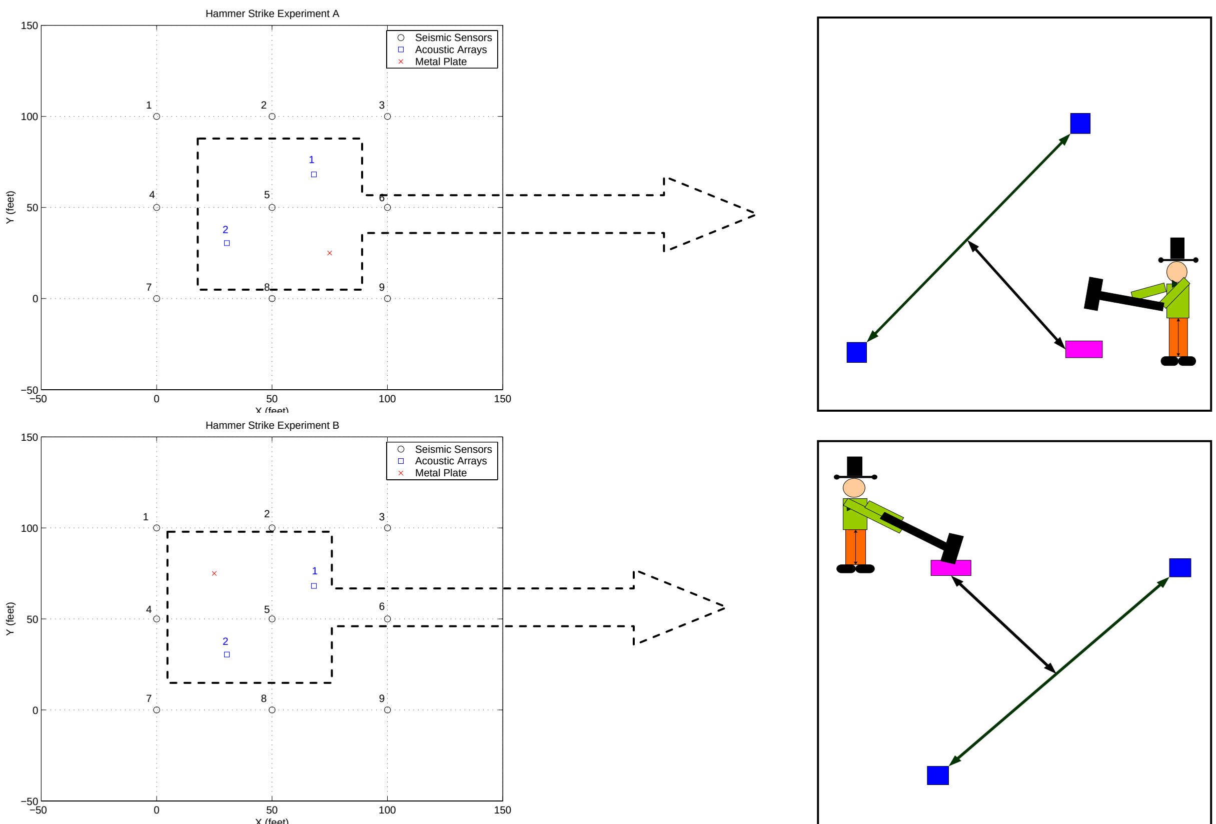

Acoustic Array Localization

Case A

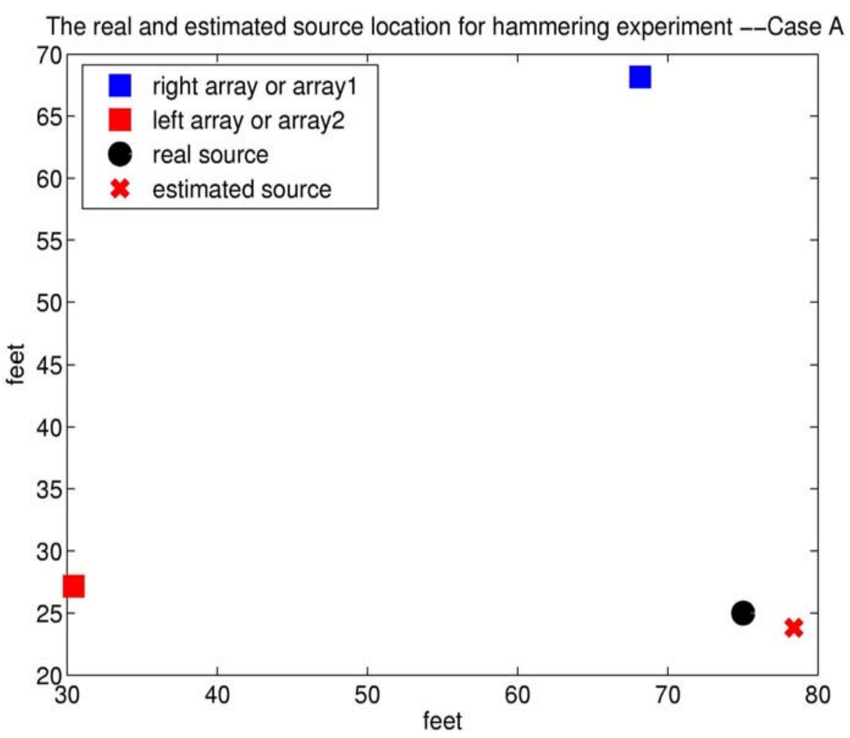

• **AML-based acoustic DOA/localization using whitening pre-processing yields metal plate at (78.4, 23.8), close to the true location of (75, 25)**

Case B

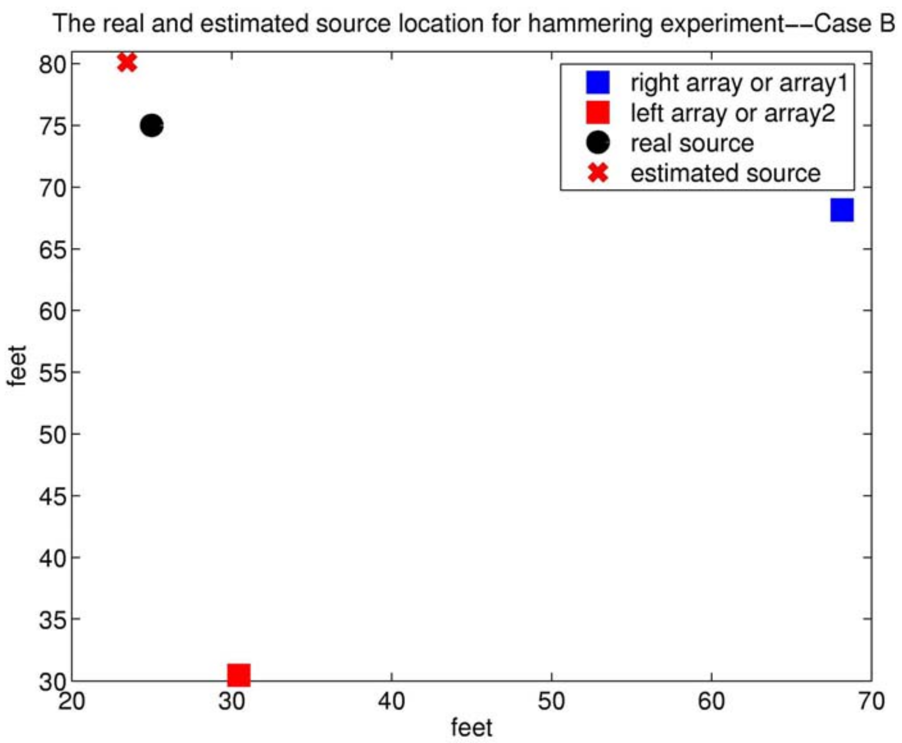

• **AML-based acoustic DOA/localization using whitening pre-processing yields metal plate at (23.4, 80.1), close to the true location of (25, 75)**

Seismic Event Detection Results

- The simple eigen-decomposition procedure can be performed on sliding time windows through the data record to find signification events of interest
- The data record with 6 significant hammer strikes was selected for analysis

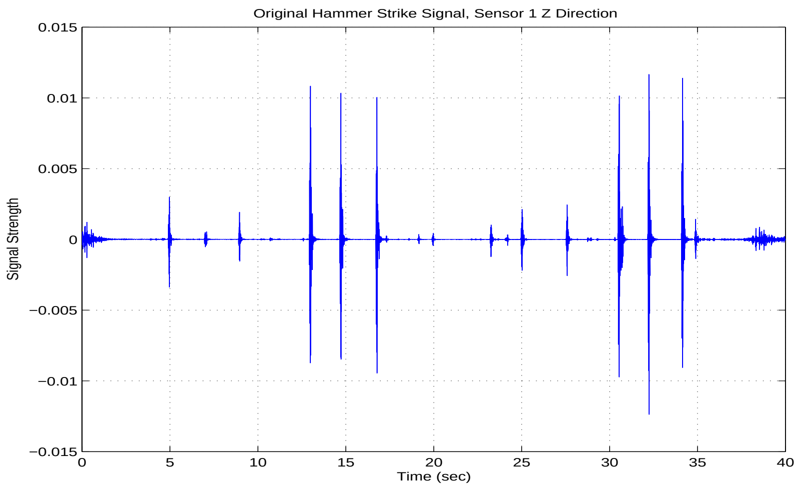

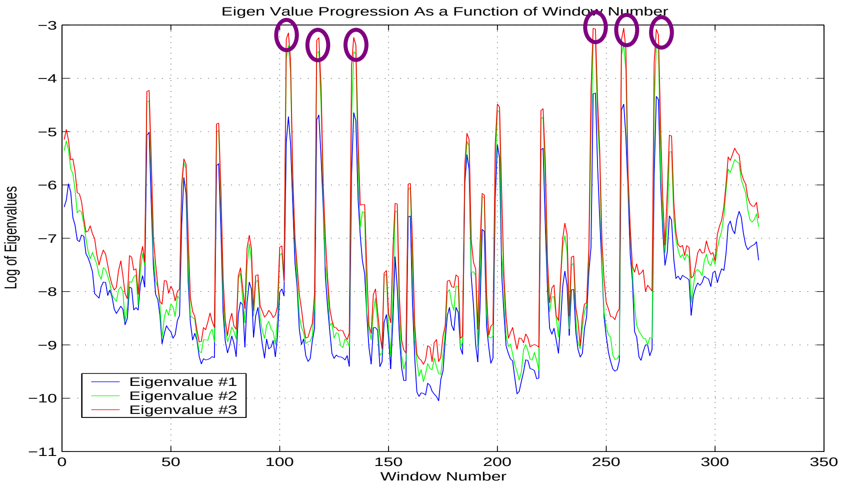

- The eigenvalue plot clearly indicates the 6 peaks above 10^{-4} is where the 6 significant hammer strikes happened

Single-Station Tri-Axial Seismic DOA Est. via Covariance Matrix Analysis

- **Use polarization analysis developed for long-range seismic data analysis**
- **The largest eigenvalue of the covariance matrix corresponds to the average energy of the strongest seismic mode polarized in the direction of the corresponding eigenvector**
- **Same can be said for the second and the smallest eigenvalues and their corresponding eigenvectors**

Single-Station Tri-Axial Seismic DOA Est. via Surface Wave Analysis

- **Rayleigh wave is elliptically polarized in two mutually orthogonal directions**

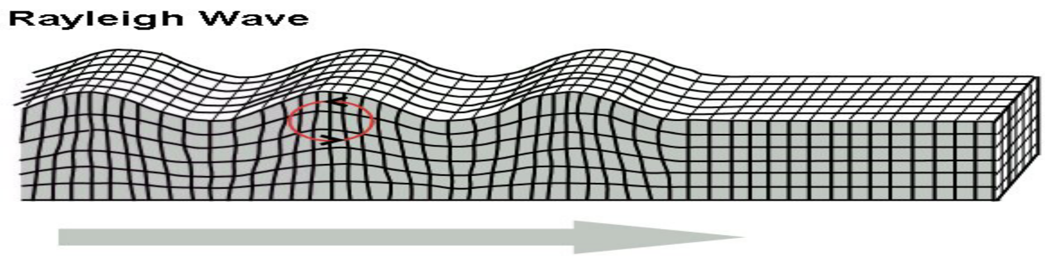

- **Love wave is rectilinearly polarized in the direction orthogonal to the two Rayleigh directions**

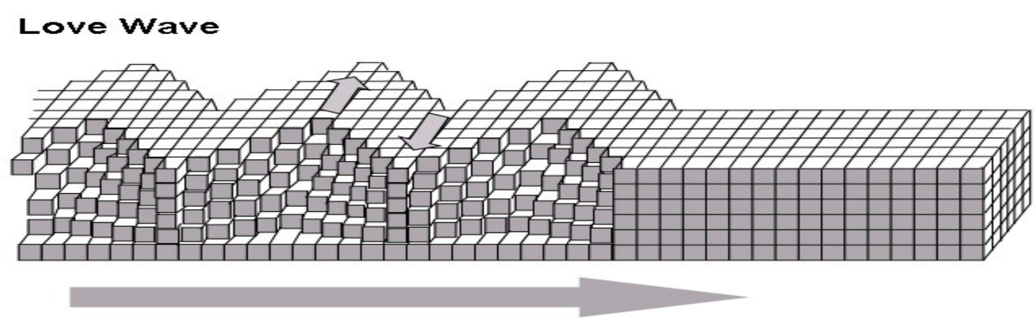

- **The three-dimensional space can be rotated such that two dimensions only pick up the Rayleigh wave, and the one other, orthogonal dimension picks up only the Love wave**

Seismic Source Localization

Covariance Analysis Source Localization

Location in **Feet**	True SrcLoc	Unw. TLS	Wt. TLS	Unw. L1	Wt. L1	S.D. Range
Hmr. A x-coordinate	75	59.15	85.43	61.48	83.07	74.35 1.71
Hmr. A y-coordinate	25	64.11	31.82	54.49	28.51	
Hmr. B x-coordinate	25	52.43	30.81	38.39	31.10	13.76 0.39
Hmr. B y-coordinate	75	79.72	81.43	81.23	84.84	

Surface Wave Analysis Source Localization

Location in **Feet**	True SrcLoc	Unw. TLS	Wt. TLS	Unw. L1	Wt. L1	S.D. Range
Hmr. A x-coordinate	75	80.31	81.27	85.20	80.64	5.99 1.66
Hmr. A y-coordinate	25	32.19	27.59	34.15	26.67	
Hmr. B x-coordinate	25	29.89	27.56	31.14	26.97	3.17 0.37
Hmr. B y-coordinate	75	69.62	77.36	65.72	79.66	

Combined Acoustic/Seismic Localization Case A

Location in Feet	X	Y
True	75	25
Acoustic	78.4	23.8
Seismic	80.6	26.7
Fusion	79.5	25.2

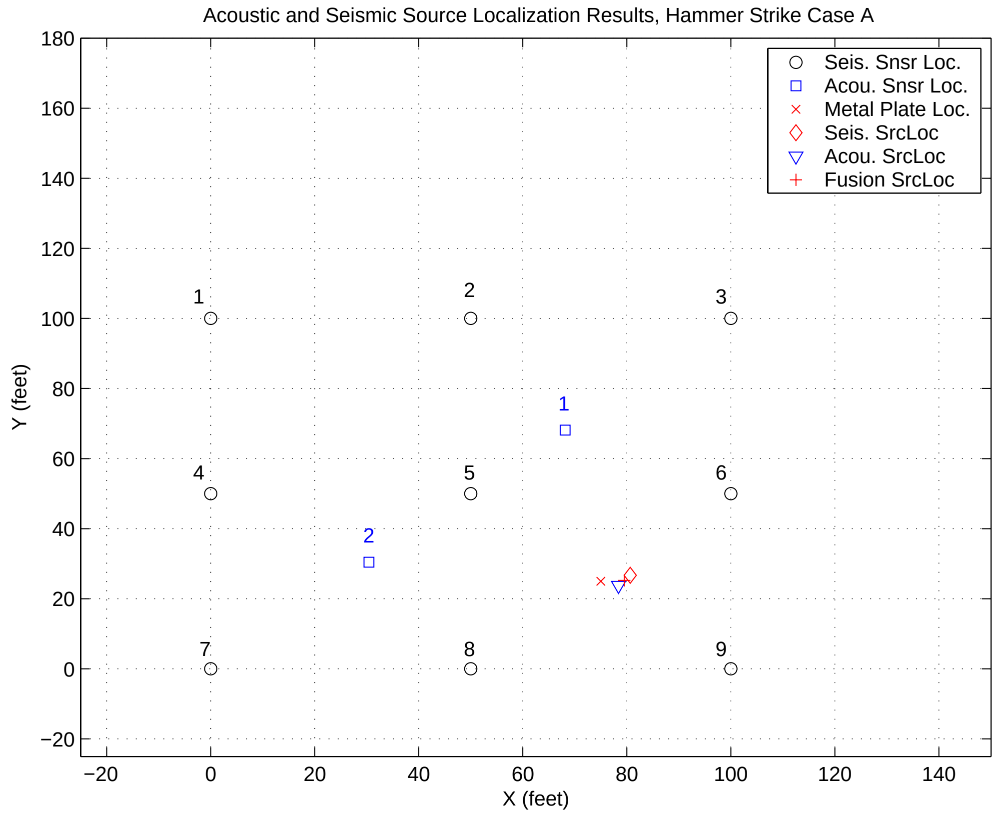

- A simple average of the acoustic and seismic coordinates gives the fusion result

Combined Acoustic/Seismic Localization Case B

Location in Feet	X	Y
True	25	75
Acoustic	23.4	80.1
Seismic	27.6	77.4
Fusion	25.5	78.7

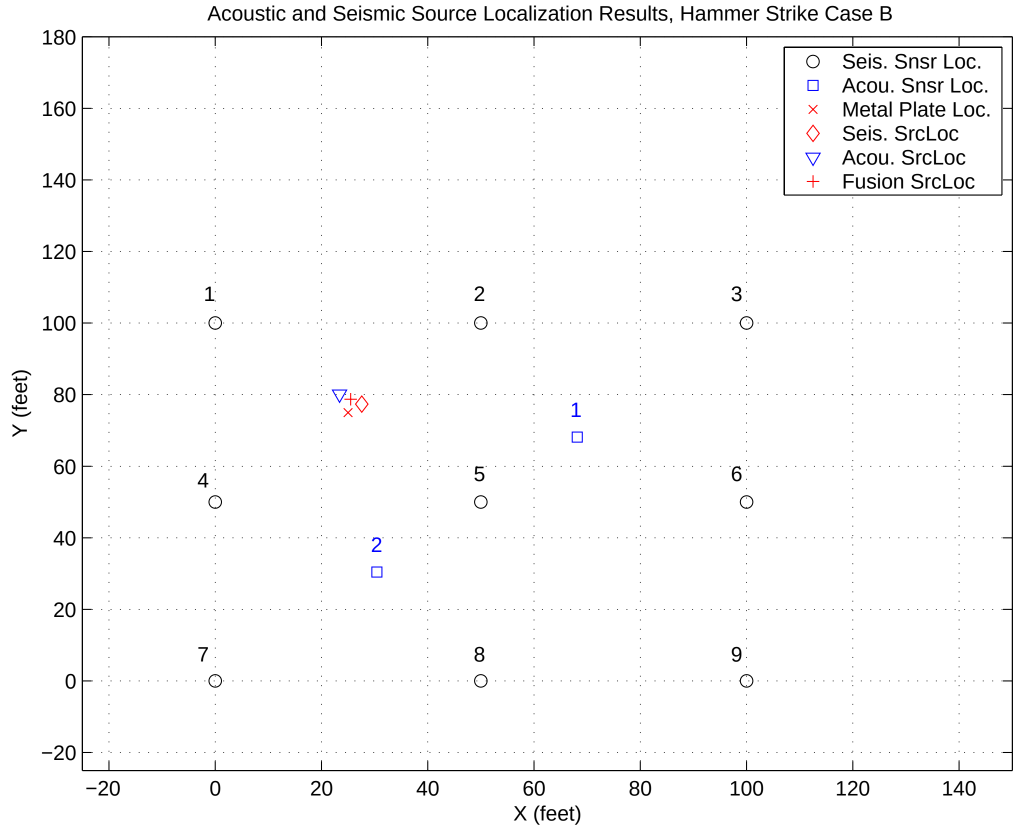

- The fusion result in this case is closer to the true source than either the acoustic or the seismic result

4. Sensor Node Localization
System Description

- *m* anchor nodes (locations known) and *n* sensor nodes (locations to be estimated)
- Each sensor node has distance measures to all of the sensor and anchor nodes in its neighborhood

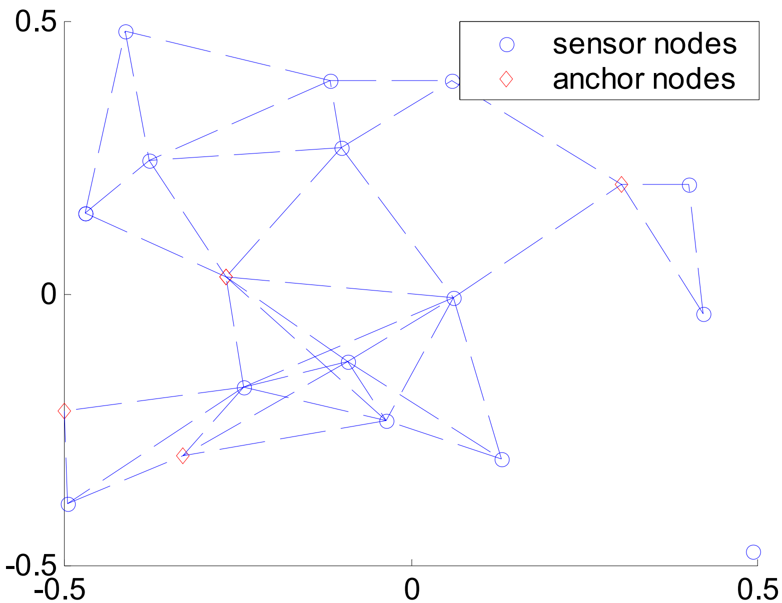

Example

- *4* anchor nodes at each corner and 15 sensor nodes in the middle
- Radio range = *0.35*
- Every link represents a communication link
- Distance measurement d_{ij} available

Metric for Minimization

$$F(\mathbf{x}) = \sum_{i,j} \left| \left\| x_i - x_j \right\|^2 - d_{ij}^2 \right|^2 + \sum_{i,k} \left| \left\| x_i - a_k \right\|^2 - d_{ik}^2 \right|^2$$

$\mathbf{x} = \left[x_1^T \quad \cdots \quad x_n^T \right]^T$ $\quad x_i \in R^2$ is the *i-th* sensor location estimate

$a_k \in R^2$ is the *k-th* anchor node location

$$\hat{\mathbf{x}} = \arg\min_{\mathbf{x}} F(x_1, x_2, \ldots, x_n),$$

d_{ij} and d_{ik} are known (estimated) range values

Centralized Method :

- Gauss-Newton (non-linear least squares)
- Multi-Dimensional Scaling
- SDP

Require communications to a central computer

Distributed Gauss-Newton Sequential/Parallel Node Localization Methods

Estimation Results

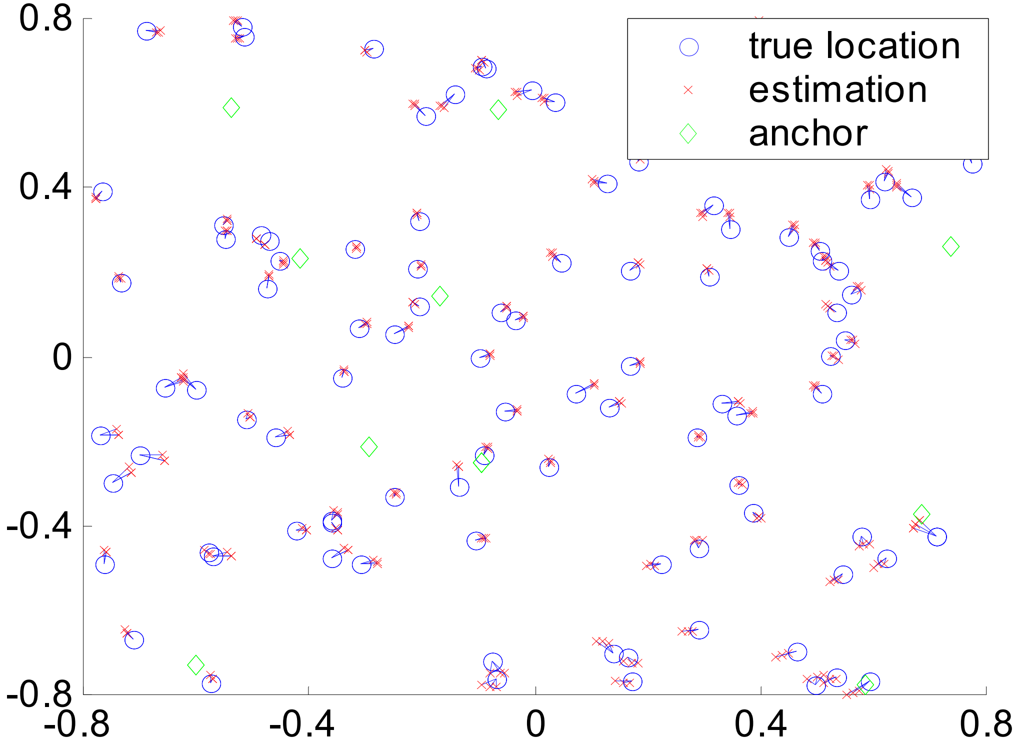

- *10* anchor nodes at each coroner and *100* sensor nodes in the middle
- Radio range = *0.35*

Some Average Iteration/ Processing Time Behaviors

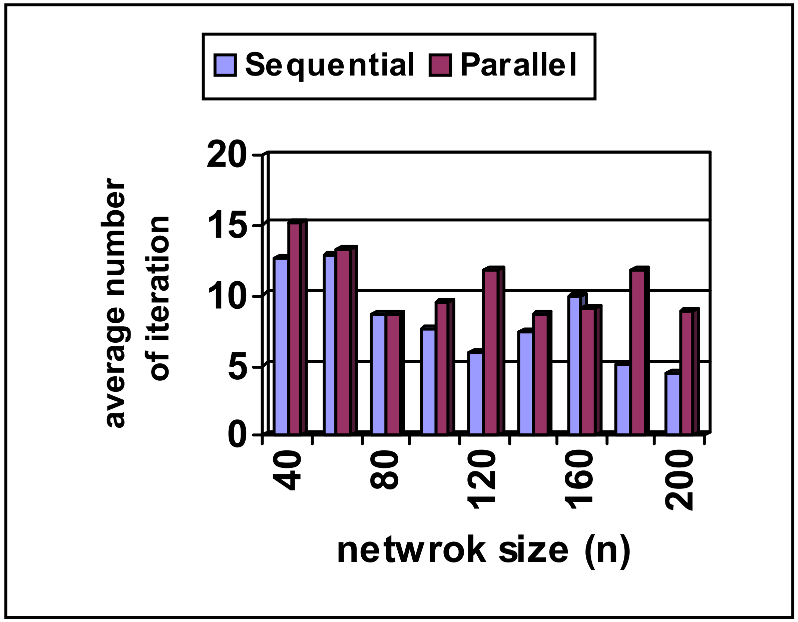

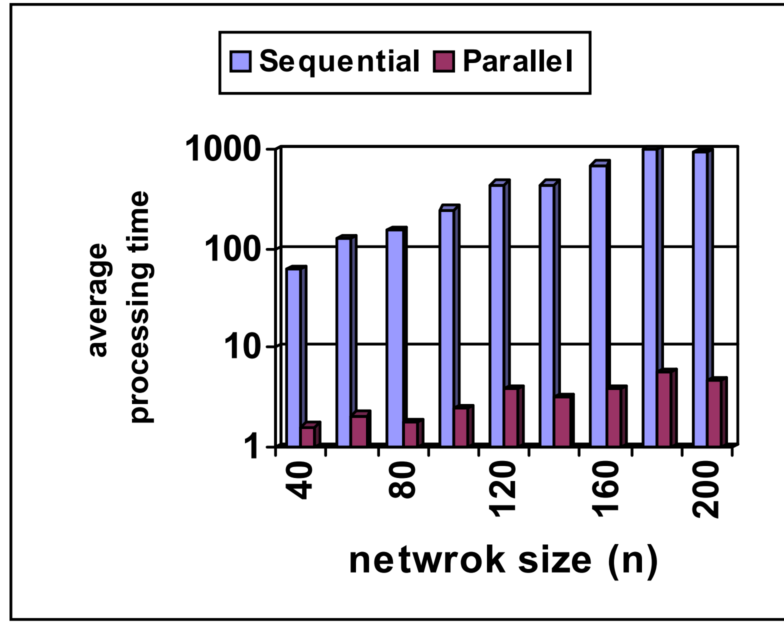

- Keep the density of the sensor, the ratio of sensor/anchor and the radio range to be constant
- Each sensor stops the algorithm if $\|p_i\| \le 0.01$

Comparison to Centralized Algorithm

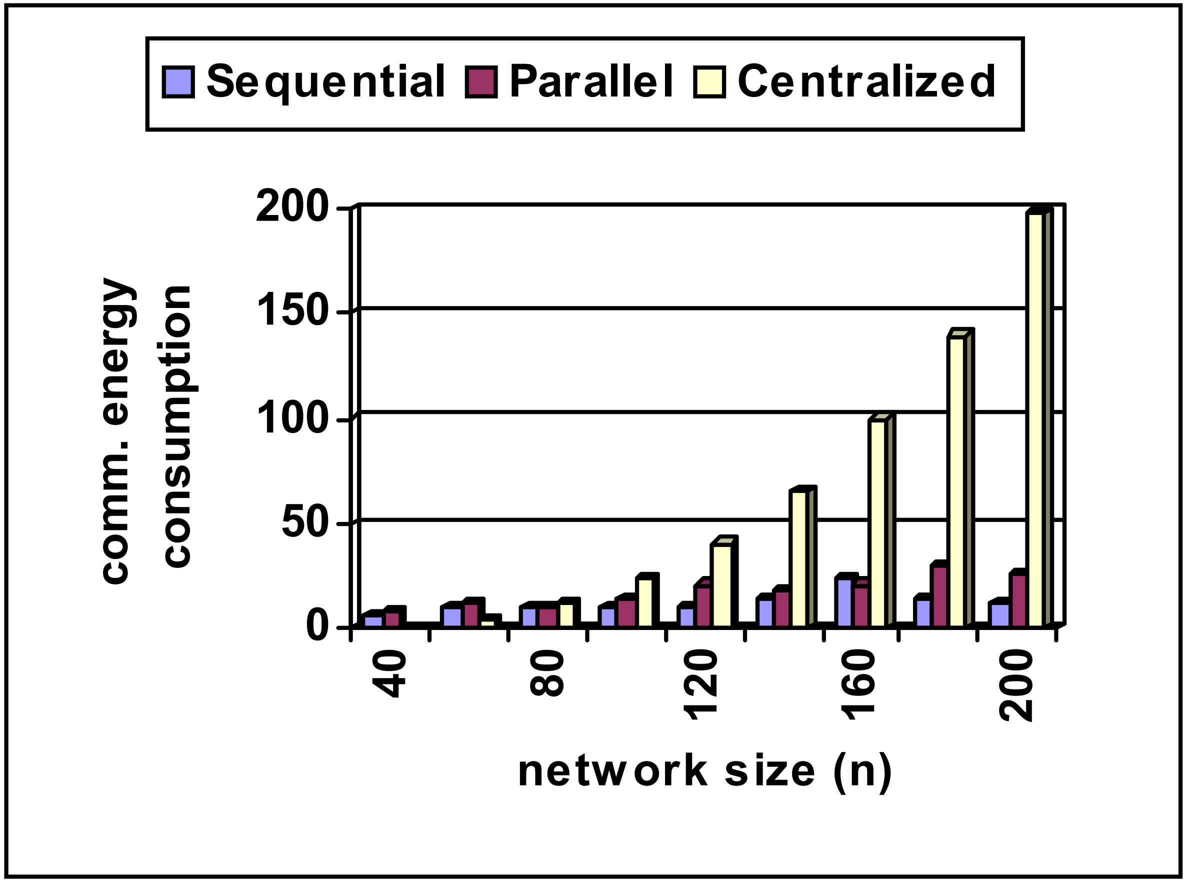

5. Conclusions

- Considered three source localization methods:
  1. TDOA-LS algorithms(centralized processing)
  2. AML algorithm (distributed processing)
  3. Seismic localization: covariance method (centralized processing) and surface wave method (distributed processing)
- Distributed Gauss-Newton Node Localization Method (Sequential and Parallel algorithms)

6. Challenging Processing Problems in SN

- Perform distributed computation of eigenvalue/ eigenvector/singular value/singular vector without sending raw data from the sensors to a central proc.
- Theoretical/practical (i.e., low complexity) use of data fusion from different types of sensors (video/acoustic/ seismic) of different quality and sampling rate
- Theoretical (e.g., CRB)/practical issues of placement of sensors of different types
- Using random set theory method for determining number of sources and nearest neighboring nodes
- Real-time/practical (i.e., low complexity) use of particle filtering methodology for source/sensor node tracking